ELSEVIER

Carbohydrate Research 337 (2002) 353–367

CARBOHYDRATE RESEARCH

www.elsevier.com/locate/carres

Quantum mechanical and NMR spectroscopy studies on the conformations of the hydroxymethyl and methoxymethyl groups in aldohexosides

Igor Tvaroška,[a,†] François R. Taravel,[b,*] Jean Pierre Utille,[b] Jeremy P. Carver[a]

[a] *GlycoDesign Inc., 480 University Avenue, Suite 400, Toronto, Ont., Canada M5G 1V2*
[b] *Centre de Recherches sur les Macromolécules Végétales, CNRS,[‡] B.P. 53, F-38041 Grenoble, France*

Received 4 October 2001; accepted 29 November 2001

Abstract

The potential energy surfaces of the hydroxymethyl and methoxymethyl groups in methyl hexopyranosides have been extensively studied, employing quantum mechanical calculations and high resolution NMR data. The structure and energy of the C-5–C-6 rotamers were calculated at the B3LYP level of the density functional theory (DFT). For all, geometry optimizations were carried out for 264 conformers of 16 methyl D-gluco- and methyl D-galactopyranoside derivatives **1**–**16** at the B3LYP/6-31G** level. For all calculated minima, single-point calculations were performed at the B3LYP/6-311 + + G** level. Solvent effects were considered using a self-consistent reaction field method. Values of the vicinal coupling constants $^3J_{\text{H-5–H-6}R}$, $^3J_{\text{H-5–H-6}S}$, $^3J_{\text{C-4–H-6}R}$, and $^3J_{\text{C-4–H-6}S}$ for methyl D-glucopyranosides, methyl D-galactopyranosides and their 6-*O*-methyl derivatives **9**–**16** were measured in two solvents, methanol and water. The calculated *gg*, *gt*, and *tg* rotamer populations of the hydroxymethyl and methoxymethyl groups in **9**–**16** agreed well with experimental data. The results clearly showed that the population of *gg*, *gt*, and *tg* rotamers is sensitive to solvent effects. It was concluded that the preference of rotamers in **1**–**16** is due to the hydrogen bonding and solvent effects.

Keywords: Quantum mechanical calculations; Conformation; Aldohexosides; NMR

1. Introduction

During oligosaccharide biosynthesis, oligosaccharides are converted into hybrid and complex oligosaccharides by the addition of 2-acetamido-2-deoxy-α-D-glucopyranosyl (GlcNAc) residues. These oligosaccharide chains of N- and O-linked glycoproteins are involved in many physiological and pathological cell processes as well, such as cancer.[1] Characterization of conformational behavior is a prerequisite to an understanding of the biological function of these carbohydrates. The conformation about the exocyclic C-5–C-6 bond is of major importance in the determination of the three-dimensional structure of these carbohydrate molecules. Although, the conformational properties around the C-5–C-6 bond has been the subject of several investigations including both experimental and theoretical studies,[2,3] the factors that determine the conformational behavior of the exocyclic C-5–C-6 linkage are still not perfectly understood.

The hydroxymethyl groups in carbohydrates usually exist in three staggered orientations (gauche–gauche, *gg*; trans–gauche, *tg*; and gauche–trans, *gt*) that correspond to local minima. In crystals,[4] the *gt* and *gg* rotamers are preferred for D-hexopyranoses, having the hydroxyl group orientation at C-4 as it is in D-glucopyranose (equatorial), while the *tg* and *gt* rotamers are preferred for those having the hydroxyl group orientation at C-4 as it is in D-galactopyranose (axial). Solu-

* Corresponding author. Tel.: + 33-4-76037640; fax: + 33-4-76547203.
E-mail address: taravel@cermav.cnrs.fr (F.R. Taravel).
† Present address: Institute of Chemistry, Slovak Academy of Sciences, Dubravska cesta 9, SK-842 38 Bratislava, Slovak Republic.
‡ Affiliated with the Joseph Fourier University of Grenoble, France.

0008-6215/02/$ - see front matter
PII: S0008-6215(01)00315-9

tion conformations of the hydroxymethyl group[2,3,5] are similar to those found in the solid state, however, very often a negative population for the *tg* conformer is reported from the analysis of NMR data. For glucopyranose derivatives, the percentage populations for the *gg*, *gt* and *tg* rotamers are 45–70%, 30–55%, and −25 to 25%, respectively. For galactopyranose derivatives, the corresponding populations are 10–25%, 55–78%, and 2–30%.

The complexity of the conformational equilibrium around the C-5–C-6 linkage is believed to be due to a combination of several factors including the gauche effect, hydrogen bonding, solvent effects, and 1,3-synaxial interactions. Theoretical calculations[6–26] have been employed to understand the role of these factors and to predict the conformational preference of the hydroxymethyl group. The calculated relative energy of the C-5–C-6 rotamers depends on the method used and usually the *tg* conformation is predicted to be the lowest energy conformation for the D-pyranoses with the gluco configuration at C-4.

Recently we have undertaken an ab initio quantum mechanical analysis of the potential energy surface for rotation of the exocyclic hydroxymethyl and methoxymethyl groups in carbohydrate model compounds.[18] We have concluded that the gauche orientation of the O-5–C-5–C-6–O-6 moiety is due to a presence of hydrogen bonding and solvent effects and not due to the gauche effect. In this paper, as an extension of our previous work, we have explored the effect of the neighboring hydroxyl group at C-4 on the conformational properties of the C-5–C-6 linkage in 16 hexopyranose derivatives using quantum mechanical methods in the gas phase and in aqueous solution. The rotamer distribution of the hydroxymethyl and methoxymethyl groups in eight derivatives of methyl glucopyranoside and methyl galactopyranoside in the gas phase and two solvents were determined using vicinal proton–proton and carbon–proton coupling constants and quantum mechanical calculations.

2. Methods

Models and computational procedures.—Conformational equilibria around the C-5–C-6 linkage were studied (Scheme 1) for methyl 2,3-dideoxy-α-D-glucopyranoside (**1**), methyl 2,3-dideoxy-β-D-glucopyranoside (**2**), methyl 6-*O*-methyl-2,3-dideoxy-α-D-glucopyranoside (**3**), methyl 6-*O*-methyl-2,3-dideoxy-β-D-glucopyranoside (**4**), methyl 2,3-dideoxy-α-D-galactopyranoside (**5**), methyl 2,3-dideoxy-β-D-galactopyranoside (**6**), methyl 6-*O*-methyl-2,3-dideoxy-α-D-galactopyranoside (**7**), methyl 6-*O*-methyl-2,3-dideoxy-β-D-galactopyranoside (**8**), methyl α-D-glucopyranoside (**9**), methyl β-D-glucopyranoside (**10**), methyl 6-*O*-methyl-α-D-glucopyranoside (**11**), methyl 6-*O*-methyl-β-D-glucopyranoside (**12**), methyl α-D-galactopyranoside (**13**), methyl β-D-galactopyranoside (**14**), methyl 6-*O*-methyl-α-D-galactopyranoside (**15**), and methyl 6-*O*-methyl-β-D-galactopyranoside (**16**). The orientations about the C-4–O-4, C-5–C-6, and C-6–O-6 bonds are described by torsion angles χ_4 [$\chi = \chi$(C-5–C-4–O-4–H-4)], [$\omega = \omega$(O-5–C-5–C-6–O-6)], and Ψ [$\Psi = \Psi$(C-5–C-6–O-

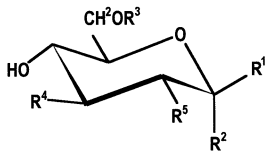

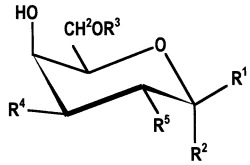

	R1	R2	R3	R4	R5
1	H	OCH_3	H	H	H
2	OCH_3	H	H	H	H
3	H	OCH_3	CH_3	H	H
4	OCH_3	H	CH_3	H	H
9	H	OCH_3	H	OH	OH
10	OCH_3	H	H	OH	OH
11	H	OCH_3	CH_3	OH	OH
12	OCH_3	H	CH_3	OH	OH

	R1	R2	R3	R4	R5
5	H	OCH_3	H	H	H
6	OCH_3	H	H	H	H
7	H	OCH_3	CH_3	H	H
8	OCH_3	H	CH_3	H	H
13	H	OCH_3	H	OH	OH
14	OCH_3	H	H	OH	OH
15	H	OCH_3	CH_3	OH	OH
16	OCH_3	H	CH_3	OH	OH

Scheme 1. Schematic representation of methyl 2,3-dideoxy-α-D-glucopyranoside (**1**), methyl 2,3-dideoxy-β-D-glucopyranoside (**2**), methyl 6-*O*-methyl-2,3-dideoxy-α-D-glucopyranoside (**3**), methyl 6-*O*-methyl-2,3-dideoxy-β-D-glucopyranoside (**4**), methyl 2,3-dideoxy-α-D-galactopyranoside (**5**), methyl 2,3-dideoxy-β-D-galactopyranoside (**6**), methyl 6-*O*-methyl-2,3-dideoxy-α-D-galactopyranoside (**7**), and methyl 6-*O*-methyl-2,3-dideoxy-β-D-galactopyranoside (**8**), methyl α-D-glucopyranoside (**9**), methyl-β-D-glucopyranoside (**10**), methyl 6-*O*-methyl-α-D-glucopyranoside (**11**), methyl 6-*O*-methyl-β-D-glucopyranoside (**12**), methyl α-D-galactopyranoside (**13**), methyl β-D-galactopyranoside (**14**), methyl 6-*O*-methyl-α-D-galactopyranoside (**15**), and methyl 6-*O*-methyl-β-D-galactopyranoside (**16**).

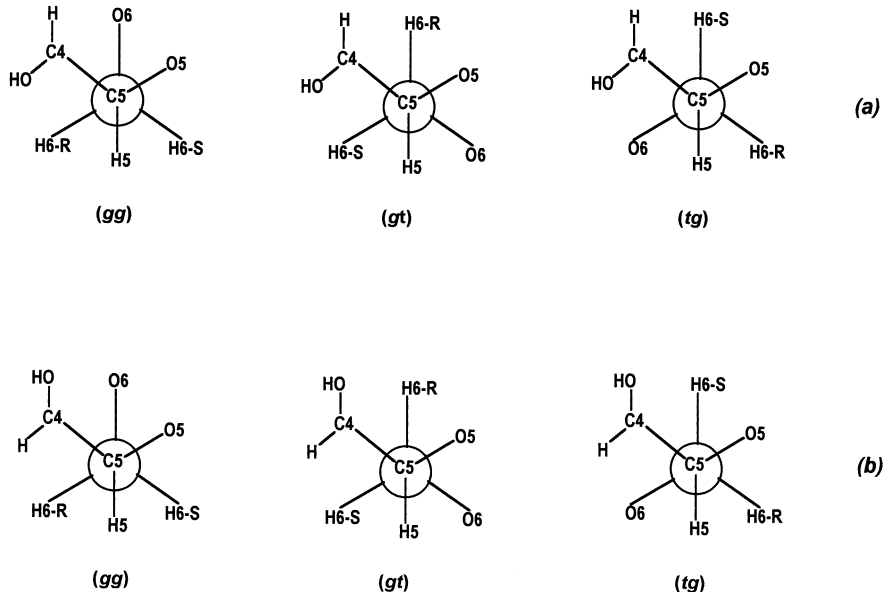

Scheme 2. Schematic representation of the *gg*, *gt*, and *tg* conformers around the C-5–C-6 bond showing the labeling of atoms for the (a) equatorial and (b) axial orientation of the C-4 hydroxyl group, respectively.

6–R3)], where R is H (in **1**, **2**, **5**, **6**, **9**, **10**, **13**, **14**) or C (in **3**, **4**, **7**, **8**, **11**, **12**, **15**, **16**), respectively. For the C-5–C-6 rotamers, we used the standard nomenclature (Scheme 2). The O-5 and C-4 are the reference atoms and staggered conformers are designated as the *gt* ($\omega \sim 60°$), *tg* ($\omega \sim 180°$), and *gg* ($\omega \sim -60°$). Three staggered orientations about the C-4–O-4 and C-6–O-6 bonds are denoted as *G* (synclinal, gauche, 60°), *T* (antiperiplanar, trans, 180°), and *MG* (−synclinal, −gauche, −60°), respectively. In the text, conformations are named using the order *gg* (or *gt*, or *tg*), χ_4 and Ψ with the definitions mentioned above, e.g., *ggGT* means that the C-5–C-6 rotamer is *gg*, the angle χ_4 has the torsional angle C-5–C-4–O-4—H-4 approximately gauche, and the angle Ψ has the torsional angle C-5–C-6–O-6–R3 approximately trans.

The ab initio calculations were carried out with the JAGUAR program.[27] The optimization of the geometry was performed employing a hybrid Hartree–Fock-density functional scheme, the adiabatic connection method—Becke three-parameter with Lee–Yang–Parr (B3LYP) functional[28]—of density functional theory (DFT)[29] with the standard 6-31G** basis set. Full optimizations were accomplished using the gradient optimization routines of the program without any symmetry constraints. The vibrational frequencies were calculated at the B3LYP/6-31G** level and the zero-point energy, thermal and entropy corrections were evaluated. Ultimately, geometries of all minima were used to calculate their single point energy with the 6-311++G** basis set. This level of theory has been shown to give reasonable potential energy surfaces for D-aldo- and D-ketohexoses and reduces the basis superposition error that is relevant for systems with hydrogen bonds.[24] The solvent effects on the conformational equilibrium have been investigated with a self-consistent reaction field method[30] as implemented in the JAGUAR program at the B3LYP/6-31G** level. Because the same approach correctly predicts the pK_a values for a large set of different molecules,[27] we expect that the solvation energies to be reasonable well predicted. Solvation calculations were carried out for two solvents, namely methanol ($\varepsilon = 33.62$) and water ($\varepsilon = 80.37$) with the geometries optimized for each solvent. Conformational energy profiles around the C-5–C-6 bond in **1**–**8** were calculated by driving the ω dihedral angle from 0 to 330° in 30° increments, while allowing the remaining geometrical parameters relax. To estimate the effect of intramolecular hydrogen bonds, we have also calculated profiles where hydrogen bonds between the hydroxyl group at C-6 and C-4 were excluded by fixing the corresponding protons in the *ap* conformation. Vicinal coupling constants were calculated for each local minimum using the Haasnoot–Altona modifications of the Karplus equation[31] for the proton–proton $^3J_{\text{H-5–H-6}}$ couplings and for the carbon–proton $^3J_{\text{C-4–H-6}}$ couplings using the equation:[32]

$$^3J_{\text{C-4–H-6}} = 5.8\cos^2(\phi) - 1.6\cos(\phi) + 0.28\sin(2\phi) - 0.02\sin(\phi) + 0.52 \quad (1)$$

Materials.—Methyl α- and β-D-glucopyranosides (**9**, **10**) and methyl α- and β-D-galactopyranosides (**13**, **14**) were commercial compounds (Sigma Chemical Co.). Methyl 6-*O*-methyl-α-D-glucopyranoside (**11**) and methyl 6-*O*-methyl-β-D-glucopyranoside (**12**) were prepared according to the method of Timell.[33] Methyl

6-*O*-methyl-α-D-galactopyranoside (**15**) and methyl 6-*O*-methyl-β-D-galactopyranoside (**16**) were prepared by the same method,[33] via methyl 2,3,4-tri-*O*-benzoyl-D-galactopyranoside derivatives. Physical constants were in agreement with literature data.[34–36]

NMR spectroscopy.—NMR spectra were obtained at 303 K on AC300 and AM400 Bruker spectrometers equipped with a process controller, variable temperature system and Aspect 3000 Computer. Samples were dissolved in D_2O (99.8% D) and freeze-dried several times to remove the residual water. Finally 40 mg/mL solutions were prepared using high quality D_2O. The same solutions were used, after D_2O evaporation, to prepare CD_3OD solutions. References for the chemical shifts were taken from standard values.[2,37–40] H-6*R* and H-6*S* were assigned according to Gagnaire et al.[41,42] and Ohrui et al.[39,43] The use of a viscous solvent (D_2O) with such concentrated solutions can cause line broadening due to relaxation phenomena and thus poorer resolution. This does not affect conformational preferences.

^1H and ^{13}C assignments were made using homo- and heteronuclear correlation spectroscopy (COSY[44] and SPI[45] experiments). COSY spectra[44] were recorded using 1024×256 data matrices and processed with zero filling in the F1 dimension. The spectral width was 1080 Hz in both dimensions. A sine-squared function was used prior to Fourier transformation. Selective population inversion experiments[45] were used to assign ^{13}C signals. Each ^{13}C signal is detected after selective inversion of one of the ^{13}C satellite peaks of the hydrogen atom directly coupled to the carbon. The selective ^1H 180 pulse was created using a DANTE sequence.[46,47] 4K data points were used in the F2 dimension. Selective 2D-J heteronuclear experiments[48] were performed to measure three-bond carbon–proton coupling constants $^3J_{C,H}$. To minimize pulse imperfection, EXORCYCLE phase cycling was used for ^{13}C pulses. The selective ^1H 180 pulse was created using a DANTE sequence.[46,47] 4K data points were used in the F2 dimension. After Fourier transformation in the F2 dimension, only the slices corresponding to ^{13}C lines of interest were treated in the F1 dimension in which no apodization functions were used.

3. Results and discussion

Conformational preferences of hydroxymethyl and methoxymethyl groups.—To shed some light into the influence of the C-4 hydroxyl group on the conformation around the C-5–C-6 bond, at first we have studied 2,3-dideoxy derivatives of methyl D-gluco- and methyl D-galactopyranoside (**1**–**8**). Conformational analysis of these compounds is a convenient way to determine the influence of hydrogen bonding and gauche effect on rotamer populations. The B3LYP6-311 + + G**//6-31G** conformational energy profiles for the rotation around the C-5–C-6 bond for α anomers (**1**, **3**, **5**, and **7**) are presented in Figs. 1 and 2, respectively. The corresponding β anomers (**2**, **4**, **6**, and **8**) showed similar profiles and data are not presented. The solid lines represent profiles calculated with full relaxation for a given value of the ω-angle. The dashed lines represent profiles calculated with the orientations of HO-4 and HO-6 hydrogens in the *ap* local minimum in order to avoid steric clashes and intramolecular hydrogen bonding. It is apparent that when the hydroxyl groups are allowed to interact by hydrogen bonding (solid lines), their conformational profiles differ significantly from those without hydrogen bonds (dashed lines) and from profiles calculated for model compounds without the C-4 hydroxyl group.[18] For **1**, the calculations predicted four minima for the torsional potential. Inspection of the optimized structures revealed that for **1**, two deep minima at $\omega = 150$ and 240° are due to the O-4–H-4···O-6 hydrogen bond. For **3**, the deep minimum at $\omega = 220°$ is a result of the O-4–H-4···O-6 hydrogen bond. A similar pattern was observed for galacto derivatives. For example, the conformational profile of **5** shows two deep minima at $\omega = 220$ and 330° that reflect the stabilization by the hydrogen bond O-6–H-6···O-4 and O-4–H-4···O-6, respectively. Unlike the op-

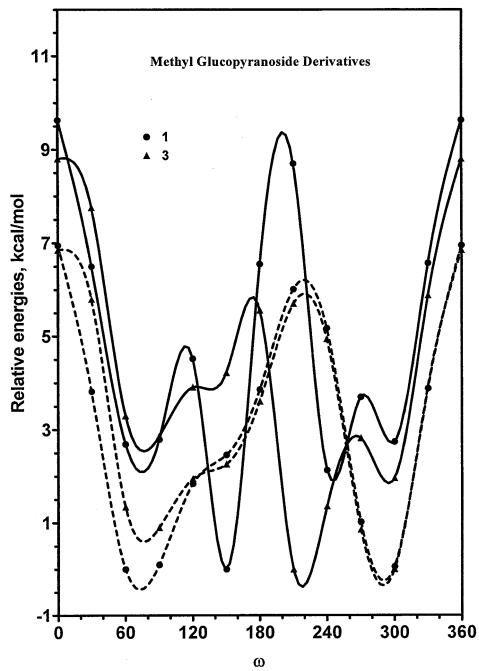

Fig. 1. Ab initio B3LYP/6-311 + + G**//6-31G** potential energy of rotation about the C-5–C-6 linkage for methyl 2,3-dideoxy-α-D-glucopyranoside (**1**, ●) and methyl 6-*O*-methyl-2,3-dideoxy-α-D-glucopyranoside (**3**, ▲) calculated with the optimized orientation (solid line) and with the *ap* orientation (dashed line) of the C-4 and C-6 hydroxyls, respectively.

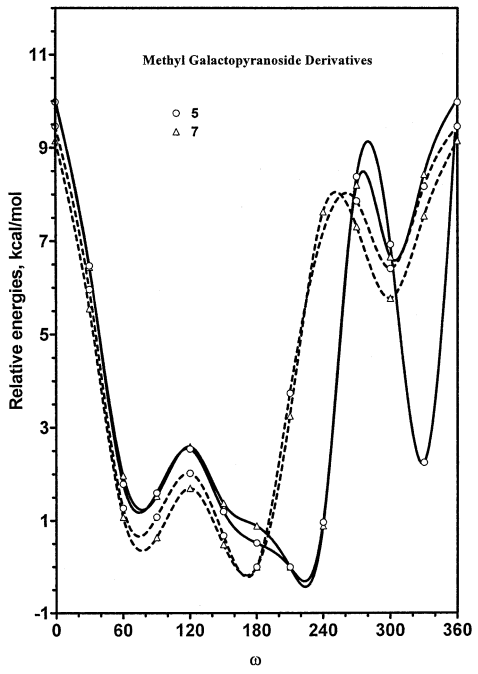

Fig. 2. Ab initio B3LYP/6-311 + + G**//6-31G** potential energy of rotation about the C-5–C-6 linkage for methyl 2,3-dideoxy-α-D-galactopyranoside (**5**, ○) and methyl 6-*O*-methyl-2,3-dideoxy-α-D-galactopyranoside (**7**, △) calculated with the optimized orientation (solid line) and with the *ap* orientation (dashed line) of the C-4 and C-6 hydroxyls, respectively.

timized profiles, the so-called *ap* profiles (dashed lines) are noticeably simpler with a threefold character and display the expected differences between the two carbohydrate models. For models with the gluco configurations at C-4 (**1**, **3**), two minima appear at $\omega = \sim 60°$ (*gt*), and $\sim -60°$ (*gg*), respectively. The *tg* rotamer ($\omega = \sim 180°$) is not present. The rotational barrier between the *gt* and *gg* conformers is approximately 6 kcal/mol and that between the *gg* and *gt* conformers is ~ 7 kcal/mol. These can be compared with 5 kcal/mol barrier estimated for D-glucose and methyl β-D-glucopyranoside from results of ultrasonic relaxation.[3,49] For models with the galacto configurations at C-4 (**5**, **7**), the deepest minimum appears at $\omega = \sim 180°$ (*tg*), the second at $\omega = \sim 60°$ (*gt*), and the third at $\omega = \sim -60°$ (*gg*). The rotational barrier between the *tg* and *gt* conformers is approximately ~ 2 kcal/mol and that between the *tg* and *gg* conformers is ~ 9 kcal/mol. The synperiplanar barrier ($\omega = 0°$) between the *gt* and *gg* conformers is similar, ~ 9 kcal/mol. All calculated barriers are similar to those previously reported for monosaccharide derivatives.[3,4,17,18,25]

These results clearly showed that the conformational profiles and conformation of hydroxymethyl moiety depends on the orientation of the HO-4 and HO-6 hydrogen atoms. Therefore, geometry optimizations were carried out for all possible minima occurring around the C-4–O-4, C-5–C-6, and C-6–O-6 linkages. On the whole, we have optimized structures of 216 conformers, 27 (3^3) for each molecule from **1**–**8**. For the generation of the starting conformation around the C-1–O-1 anomeric bond, we used the one that corresponds to the conformer predicted by the exo-anomeric effect.[50] The energies (ΔE) of the resulting local minima were calculated at the B3LYP/6-3111 + + G**//6-31G** level. The B3LYP/6-31G** solvation energies, zero-point vibrational energies, the thermal energies, and the entropies together with the ΔE values were utilized to give estimates of ΔG_{gas} and ΔG_W. The results are given in Tables 1–4 together with observed hydrogen bonds.

As can be seen from Tables 1–4, the optimization of the 27 starting structures at the B3LYP/6-31G ** level led to 22 distinct minima for compounds with the hydroxyl group at C-6 (**1**, **2**, **5**, **6**) and to 18 minima for compounds with the methoxyl group at C-6 (**3**, **4**, **7**, **8**), respectively. The relative energy of all 160 minima, with the exception of four, cover a relatively small interval of 7 kcal/mol. This together with rotational energy profiles (Figs. 1 and 2) implies that the potential energy surface about the ω, χ_4, and Ψ dihedral angles is very flat. Thus, interactions within a molecule or with medium (solvent, protein, etc.) can change the conformational preferences around these linkages quite significantly.

Inspection of the three-dimensional structure of conformations of **1**–**8** reveals the presence of stabilizing interactions between two hydroxyl groups or the C-6 hydroxyl group and the ring oxygen in several conformers, i.e., O-4–H···O-6, O-6–H···O-4, or O-6–H···O-5 hydrogen-bonding interactions. The two latter hydrogen bond interactions are not present in 6-*O*-methyl derivatives. Among the low energy conformers, distinct hydrogen bonding patterns are observed. Apparently, these patterns are closely related to the conformation observed around the C-5–C-6 linkage (the ω dihedral angle). For instance, all four conformers (*tgGG*, *tgMGMG*, *tgMGT*, and *tgTG*) of **1** and **2** (Table 1) with the *tg* orientation around the C-5–C-6 linkage display hydrogen-bonding interactions. The stabilizing effect on the relative energy of these conformers is immediately evident by a comparison with the corresponding 6-*O*-methyl derivatives (**3**, **4**), where the O-6-H···O-4 interactions are not present (Table 2). For the *ggGG* rotamer in **5** and **6**, the O-6–H group forms hydrogen bonds with both the ring oxygen and the O-4–H group, while it only forms one hydrogen bond in **7** and **8**. The extra hydrogen bond makes the *ggGG* conformer significantly more favorable than other conformers compared to **7** and **8**, where the preferred conformer is *ggGT*. The geometrical parameters for the hydrogen bond interactions are in a range $d_{O\cdots O} = 2.7–3.1$ Å and $d_{H\cdots O} = 1.9–2.4$ Å. Clearly, the relative energies of con-

Table 1
Relative energies (ΔE, kcal/mol), free energies in vacuum (ΔG_{gas}), aqueous solution (ΔG_W) and observed hydrogen bonds calculated for **1** and **2** using the B3LYP/6-311++G**//6-31G** method

	Methyl 2,3-dideoxy-α-D-glucopyranoside (**1**)			Methyl 2,3-dideoxy-β-D-glucopyranoside (**2**)			Hydrogen bond
	ΔE	ΔG_{gas}	ΔG_W	ΔE	ΔG_{gas}	ΔG_W	
ggGG	0.55	0.73	1.55	1.19	1.32	1.76	O-6–H-6···O-5
ggGMG	2.90	3.02	3.06	3.79	3.92	3.49	
ggGT	3.58	3.14	1.16	4.41	3.93	1.47	
ggMGG	0.00 [a]	0.00	0.80	0.00 [b]	0.04	1.16	O-6–H-6···O-5
ggMGMG	5.16	4.47	1.68	5.33	4.73	2.11	
ggMGT	2.64	2.34	2.23	2.98	2.73	2.73	O-4–H-4···O-6
ggTG	0.42	0.05	1.12	0.38	0.00	1.16	O-6–H-6···O-5
ggTMG	2.94	3.10	3.57	3.47	3.69	4.02	
ggTT	3.46	2.52	0.80	3.69	2.86	1.07	
gtGG	3.55	2.98	0.90	4.02	3.12	0.86	
gtGMG	0.38	0.63	0.78	0.81	0.73	0.00	O-6–H-6···O-5
gtGT	2.93	2.02	0.63	3.33	2.36	0.58	
gtMGG	4.27	3.64	1.09	4.12	3.14	0.86	
gtMGMG	1.12	1.23	1.14	1.03	0.83	0.37	O-6–H-6···O-5
gtMGT	4.13	2.47	0.00	4.08	2.65	0.22	
gtTG	3.30	2.61	0.83	3.35	2.38	0.78	
gtTMG	0.49	0.53	0.76	0.44	0.21	0.02	O-6–H-6···O-5
gtTT	3.19	1.77	0.15	3.24	1.99	0.28	
tgGG	0.35	0.91	1.44	1.00	1.58	1.77	O-6–H-6···O-4
tgMGMG	0.29	0.82	1.12	0.45	1.03	1.12	O-4–H-4···O-6
tgMGT	0.17	0.23	0.51	0.15	0.29	0.68	O-4–H-4···O-6
tgTG	0.31	0.48	0.94	0.63	0.92	1.19	O-6–H-6···O-4

[a] $E = -576.224195$.
[b] $E = -576.223316$.

formations around the C-5–C-6 linkage are influenced by hydrogen bonds. However, it is noteworthy that the relative energy of several conformers displaying hydrogen bonds is rather high. This suggests that the hydrogen bond in these conformers is weak and other factors decrease the stability of conformers.

The relative importance of hydrogen bonds on the stability of individual conformers reflects also in the calculated populations of *gg*, *gt*, and *tg* rotamers that are given in Table 5. The calculations clearly show that the *tg* conformation of the C-5–C-6 dihedral angle is the most favored in O-6-methylated compounds (**3**, **4**). Two conformers of the *tg* rotamer (*tgMGMG* and *tgMGT*) are stabilized by the O-4–H-4···O-6 hydrogen bond. On the other hand, *gt* and *gg* conformers are stabilized by hydrogen bonds compared to the *tg* conformation around the C-5–C-6 bond in **1** and **2**. The populations of the *gg*, *gt*, and *tg* rotamers calculated in vacuum from the ΔG_{gas} values for **1** and **2** are very similar 46.6:20.6:32.8 and 46.3:29.8:23.9, respectively. The same procedure employed for **3** and **4** yielded a distribution of 8.2:7.2:84.6 and 4.5:6.9:88.6, respectively. Though, the effect of solvent on the stability of rotamers depends on the character of the O-6 group, it is very similar for all four compounds (**1**–**4**). The solvent effect stabilizes the *gt* rotamer at the expense of the *gg* and *tg* rotamers for **1** and **2**. For **3** and **4**, the solvent favored the *gg* and *gt* rotamers compared to the *tg* one. As a result, the calculated distribution of rotamers for **1**, **2**, **3**, and **4** in aqueous solution is 18.5:65.1:16.4, 10.1:79.4:10.5, 29.1:47.3:23.4, and 23.5:56.7:19.7, respectively. Interestingly, these values are in reasonable agreement with the population distributions for glucopyranose derivatives of 45–70%, 30–55%, and −25 to 25%.

The presence of the *tg* rotamers in galactopyranosides is often rationalized as arising from solvent effect or unfavorable 1,3-diaxial interactions in the *gg* rotamer. Our results on **5**–**8** show that internal hydrogen bonds between the O-6 and O-4 hydroxyl groups favor the *gg* rotamer in vacuum regardless of the fact that they contain 1,3-diaxial interactions. Employing the calculated ΔG_{gas} values, estimated distribution of the *gg*, *gt*, and *tg* rotamers for **5**–**8** is 78.5:11.6:9.9, 50.5:35.8:13.6, 57.4:13.9:28.7, and 21.2:30.6:49.2, respectively. Solvent effect changes these populations to 8.6:39.4:52.0, 4.0:60.7:35.3, 24.7:59.3:16.0, and 7.0:71.5:21.5, which may be compared with experimen-

Table 2
Relative energies (ΔE, kcal/mol), free energies in vacuum (ΔG_{gas}), aqueous solution (ΔG_W) and observed hydrogen bonds calculated for **3** and **4** using the B3LYP/6-311++G**//6-31G** method

	Methyl 6-*O*-methyl 2,3-dideoxy-α-D-glucopyranoside (**3**)			Methyl 6-*O*-methyl 2,3-dideoxy-β-D-glucopyranoside (**4**)			Hydrogen bond
	ΔE	ΔG_{gas}	ΔG_W	ΔE	ΔG_{gas}	ΔG_W	
ggGG	4.06	3.74	2.72	4.68	4.34	2.99	
ggGT	3.33	2.72	0.58	4.19	3.45	0.63	
ggMGG	2.77	2.82	2.93	2.85	2.94	3.55	
ggMGT	2.34	2.04	1.54	2.71	2.42	1.94	O-4–H-4···O-6
ggTG	3.67	2.59	1.96	3.66	3.34	2.92	
ggTT	3.07	1.94	0.03	3.45	2.25	0.03	
gtGG	4.45	3.90	1.35	5.14	4.28	1.56	
gtGMG	3.71	3.27	2.18	4.32	3.59	1.39	
gtGT	2.61	2.05	0.32	3.18	2.32	0.12	
gtMGG	5.31	4.54	1.25	5.45	4.40	1.43	
gtMGMG	4.74	3.82	2.12	4.85	4.11	1.56	
gtMGT	3.76	2.94	0.38	3.77	2.67	0.09	
gtTG	4.39	3.62	1.07	4.68	3.69	1.27	
gtTMG	3.83	3.14	2.19	4.22	3.16	1.20	
gtTT	2.84	1.95	0.15	2.98	1.92	0.00	
tgMGMG	1.36	1.61	1.49	1.57	1.80	1.70	O-4–H-4···O-6
tgMGT	0.00 [a]	0.00	0.00	0.00 [b]	0.00	0.01	O-4–H-4···O-6
tgTT	5.62	4.10	1.47	5.68	4.17	1.41	

[a] $E = -615.535376$.
[b] $E = -615.534599$.

tally observed rotameric distribution for galactopyranose derivatives of 10–25%, 55–78%, and 2–30%.

The results of conformational analysis of **1**–**8** clearly show that the population of the *gg*, *gt*, and *tg* rotamers in the gas phase and aqueous solution differ considerably. Moreover, a calculation of the rotamer populations comparable with available experimental data can be only obtained when solvent contributions are included into calculations. Finally, the results demonstrate that a preference of the O-5–C-5–C-6–O-6 structural moiety for the gauche conformation (the *gg* and *gt* rotamers) is due to the intramolecular hydrogen bonding and solvent effects and not due to a stereoelectronic effect known as the gauche effect.[51]

Conformation of hydroxymethyl and methoxymethyl groups in methyl gluco- and galactopyranosides.—The rotamer populations of hexapyranosides in solution have been primarily determined by NMR spectroscopy using proton–proton coupling constants $^3J_{H\text{-}5\text{–}H\text{-}6}$, while vicinal carbon–proton coupling constants $^3J_{C\text{-}4\text{–}H\text{-}6}$ were used rarely. Here we measured both the proton–proton and carbon–proton constants to estimate the rotamer populations of eight derivatives (**9**–**16**) in two solvents, namely methanol and water. Values of the vicinal coupling constants from the analysis of the NMR spectra of **9**–**16** in both solvents are listed in Table 6, together with their predicted values from the calculated free energies of rotamers. The rotamer populations around the C-5–C-6 bond can be estimated from the two vicinal proton–proton $^3J_{H\text{-}5\text{–}H\text{-}6}$ or carbon–proton $^3J_{C\text{-}4\text{–}H\text{-}6}$ coupling constants values and the values of corresponding coupling constant for each rotamer.[2] The values of these $^3J_{H\text{-}5\text{–}H\text{-}6}$ and $^3J_{C\text{-}4\text{–}H\text{-}6}$ coupling constants can be calculated from their respective Karplus-like equations[31,52] if the geometries of the rotamers are known. For this purpose, we have calculated conformational equilibria and the structures of rotamers around the C-5–C-6 linkage of **9**–**16** employing the same approach as for **1**–**8**. The conformations and energies of **9**–**16** are reported in Table 7. The torsional angles calculated for minima and the coupling constants obtained from them using angular Karplus-type equations[31,32] are listed in Table 8, and the comparison of the predicted *gg*, *gt*, and *tg* rotamer populations with available experimental data is given in Table 9.

Potential energy surfaces of several monosaccharides have been partially studied by quantum mechanical calculations.[6–26] These studies demonstrate that the relative energies of the various conformers of hexopyranoses vary with the change of the basis set and correlation levels. Recent results[24] indicate that the DFT/B3LYP/6-311++G**//B3LYP/6-31G** level is the adequate choice for evaluating the potential energy surfaces of cyclic hexopyranoses. The conformational

energy surfaces of methyl glucopyranoside (**9**–**12**) and methyl galactopyranoside (**13**–**16**) derivatives are considerably more complex compared to the above-discussed 2,3-dideoxy derivatives (**1**–**8**). Given rotational freedom of the hydroxyl groups, there are hundreds of possible conformers. However, it has been shown that this complexity can be greatly reduced when intramolecular hydrogen bonds are considered. Their energy contribution is an important factor for the determination of the conformational energy surface of monosaccharides. It has been shown[12,13,16,20,22] that the clockwise (*C*) and counterclockwise (*CC*) networks are preferred hydrogen pattern in hexopyranoses. The cooperative effect of these hydrogen bonds significantly favors corresponding conformations of glucopyranose and galactopyranose in the gas phase. Therefore, in this work the starting rotamers around the C-5–C-6 linkage in **9**–**16** were restricted to those conformations with cooperative arrangement of hydrogen bonds and with a pyranoid ring in the $^4C_1$ conformation. Thus, for each rotamer around the C-5–C-6 bond, the clockwise (*C*) and counterclockwise (*CC*) hydrogen bond networks have been investigated. To provide insight on the importance of the solvent effects stability of the conformers, we have calculated solvation energies in methanol and water for all conformers of **9**–**16** at the B3LYP/6-31G** level using the JAGUAR program.[27] These results, together with the calculated zero-point vibrational energies, thermal energies and entropies at the 6-31G** level were combined with the ΔE values calculated at the B3LYP/6-31**G++//B3LYP/6-31G** level to give estimates of the free energies in the gas phase (ΔG_{gas}), methanol (ΔG_M), and water (ΔG_W), respectively.

The relative energies of **9**–**16** in the gas phase and two solvents are reported in Table 7 and relevant torsional angles used for calculations of vicinal coupling constants are given in Table 8. It may be seen from Table 7 that the energies of rotamers of each methyl glycoside are all within a range of less than 6 kcal/mol. Note that α anomers are always more stable than corresponding β anomers. It is evident that thermodynamics and solvation contributions to the free energy of each conformer influence their conforma-

Table 3
Relative energies (ΔE, kcal/mol), free energies in vacuum (ΔG_{gas}), aqueous solution (ΔG_W) and observed hydrogen bonds calculated for **5** and **6** using the B3LYP/6-311++G**//6-31G** method

	Methyl 2,3-dideoxy-α-D-galactopyranoside (**5**)			Methyl 2,3-dideoxy-β-D-galactopyranoside (**6**)			Hydrogen bond
	ΔE	ΔG_{gas}	ΔG_W	ΔE	ΔG_{gas}	ΔG_W	
ggGG	0.00 [a]	0.00	2.65	0.00 [b]	0.00	2.59	O-4–H-4···O-6 O-6–H-6···O-5
ggGT	3.08	1.94	1.27	3.36	2.12	1.44	O-4–H-4···O-6
ggMGMG	3.16	3.02	3.59	2.31	2.27	3.09	O-6–H-6···O-4
ggTMG	3.74	2.80	1.52	3.99	3.00	1.75	O-6–H-6···O-4
ggTT	11.13	9.21	3.74	11.34	9.38	3.91	
gtGG	6.55	4.54	1.46	6.53	4.43	1.46	
gtGMG	3.15	1.94	1.95	3.01	1.50	0.80	
gtGT	6.02	4.19	1.42	6.06	4.07	1.02	
gtMGG	4.81	3.80	2.07	3.85	2.52	1.24	
gtMGMG	2.05	1.73	2.29	1.08	0.40	0.87	
gtMGT	3.92	2.20	1.28	3.06	1.51	0.83	
gtTG	6.23	4.43	0.82	6.21	4.25	0.73	
gtTMG	3.02	2.01	1.52	2.95	1.66	0.43	
gtTT	5.24	3.64	0.81	5.26	3.45	0.35	
tgGMG	3.77	2.75	2.53	3.93	2.95	2.52	O-4–H-4···O-6
tgGT	3.57	2.57	2.51	3.53	2.54	2.39	O-4–H-4···O-6
tgMGG	2.66	2.10	2.95	1.78	1.35	2.86	O-6–H-6···O-4
tgMGMG	4.21	3.16	2.10	3.36	2.42	1.62	
tgMGT	3.52	2.40	1.87	2.49	1.50	1.43	
tgTG	3.65	2.93	2.86	3.52	2.81	2.65	O-6–H-6···O-4
tgTMG	5.06	3.21	1.10	5.15	3.26	0.90	
tgTT	4.54	1.79	0.00	4.49	1.76	0.00	

[a] $E = -576.226050$.
[b] $E = -576.224062$.

Table 4
Relative energies (ΔE, kcal/mol), free energies in vacuum (ΔG_{gas}), aqueous solution (ΔG_W) and observed hydrogen bonds calculated for **7** and **8** using the B3LYP/6-311++G**//6-31G** method

	Methyl 6-*O*-methyl-2,3-dideoxy-α-D-galactopyranoside (**7**)			Methyl 6-*O*-methyl-2,3-dideoxy-β-D-galactopyranoside (**8**)			Hydrogen bond
	ΔE	ΔG_{gas}	ΔG_W	ΔE	ΔG_{gas}	ΔG_W	
ggGG	0.23	0.88	2.87	0.40	1.33	3.87	O-4–H-4···O-6
ggGT	0.00 [a]	0.00	0.20	0.34	0.49	1.00	O-4–H-4···O-6
ggTG	7.08	6.61	5.81	7.11	6.76	6.64	
ggTT	8.00	6.94	2.76	8.45	7.52	3.40	
gtGG	5.06	4.20	1.88	5.25	4.40	2.64	
gtGMG	3.91	3.01	2.17	4.17	3.24	1.94	
gtGT	3.22	2.18	0.51	3.19	2.18	0.56	
gtMGG	3.18	3.09	2.22	2.56	2.37	2.45	
gtMGMG	2.51	2.57	3.13	1.64	2.45	3.11	
gtMGT	1.13	0.99	1.02	0.42	0.21	0.67	
gtTMG	3.45	2.68	1.69	3.76	2.74	1.07	
gtTT	2.55	1.79	0.00	2.63	1.80	0.00	
tgGMG	2.35	2.31	2.94	2.60	2.82	3.56	O-4–H-4···O-6
tgGT	0.98	0.86	1.44	1.12	1.18	2.08	O-4–H-4···O-6
tgMGMG	2.78	2.56	2.19	2.05	2.05	2.30	
tgMGT	0.97	0.70	1.10	0.00 [b]	0.00	1.23	
tgTMG	3.77	2.82	1.43	3.96	3.11	1.84	
tgTT	2.62	2.06	1.31	1.99	1.15	0.60	

[a] $E = -615.533269$.
[b] $E = -615.531427$.

tional equilibrium. Our study clearly showed that based on the ΔG_{gas} values, the counterclockwise conformation is preferred for all compounds in the gas phase. Examination of data in Table 7 revealed that although variations in the thermodynamic contributions between conformers of a given compound is not large, usually within 2 kcal/mol, it is sufficient to change the conformational preference. Accordingly, the gas phase relative free energies (ΔG_{gas}) differ from the gas phase relative energies (ΔE). The reason for the counterclockwise preference is presumably due to the presence of the anomeric methoxyl group. The aglycon methyl group favors the gauche orientation with respect to the ring oxygen due the exo-anomeric effect.[50] Moreover, contrary to the situation with free hexopyranoses, the glycosidic methoxy group can only be involved in one hydrogen bond in which it serves as the acceptor. Solvation energies show a similar variability of 3 kcal/mol with differing conformations. As a consequence, the rotamer preference of all eight methyl hexopyranosides is considerably shifted going from the gas phase to methanol and water.

The *gg*, *gt*, and *tg* rotamer populations calculated from the free energy values and the available experimental data are compared in Table 9. For methyl glucopyranosides **9** and **10**, we found that in the gas

Table 5
Rotamer populations of compounds **1**–**8** in gas phase and aqueous solution estimated from the free energies, ΔG_{gas} and ΔG_W, calculated using the B3LYP/6-311++G** method

	α Anomer			β Anomer		
	GG	*GT*	*TG*	*GG*	*GT*	*TG*
*Methyl 2,3-dideoxy-D-glucopyranosides (**1**, **2**)*						
Gas phase	46.6	20.6	32.8	46.3	29.8	23.9
Water	18.5	65.1	16.4	10.1	79.4	10.5
*Methyl 6-O-methyl-2,3-dideoxy-D-glucopyranosides (**3**, **4**)*						
Gas phase	8.2	7.2	84.6	4.5	6.9	88.6
Water	29.3	47.3	23.4	23.5	56.7	19.7
*Methyl 2,3-dideoxy-D-galactopyranosides (**5**, **6**)*						
Gas phase	78.5	11.6	9.9	50.6	35.8	13.6
Water	8.6	39.4	52.0	4.0	60.7	35.3
*Methyl 6-O-methyl-2,3-dideoxy-D-galactopyranosides (**7**, **8**)*						
Gas phase	57.4	13.9	28.7	21.2	30.6	49.2
Water	24.7	59.3	16.0	7.0	71.5	21.5

Thermodynamics and solvent effect contributions were calculated at the B3LYP/6-31G** level.

Table 6
Comparison of the vicinal $^3J_{C\text{-}4\text{–}H\text{-}6}$ (± 0.5 Hz) and $^3J_{H\text{-}5\text{–}H\text{-}6}$ (± 0.1 Hz) coupling constants (Hz) observed from the analysis of the NMR spectra of **9**–**16** with the calculated values [a]

	Methanol				Water			
	$^3J_{C\text{-}4\text{–}H\text{-}6R}$	$^3J_{C\text{-}4\text{–}H\text{-}6S}$	$^3J_{H\text{-}5\text{–}H\text{-}6R}$	$^3J_{H\text{-}5\text{–}H\text{-}6S}$	$^3J_{C\text{-}4\text{–}H\text{-}6R}$	$^3J_{C\text{-}4\text{–}H\text{-}6S}$	$^3J_{H\text{-}5\text{–}H\text{-}6R}$	$^3J_{H\text{-}5\text{–}H\text{-}6S}$
Methyl α-D-glucopyranoside (**9**)								
Obsd.	1.15	2.6	5.5	2.4	1.1	2.9	5.4	2.2
Calcd	1.8	5.2	4.1	4.0	1.7	4.4	5.3	3.7
Methyl β-D-glucopyranoside (**10**)								
Obsd.	1.2	2.5	5.25	1.95	1.0	2.4	5.9	2.0
Calcd	1.5	5.4	4.0	3.6	1.5	4.7	5.0	3.5
Methyl 6-O-methyl-α-D-glucopyranoside (**11**)								
Obsd.	1.0	2.0	4.7	1.6	1.15	2.9	4.5	2.1
Calcd	1.9	4.1	5.3	3.7	1.2	5.9	3.5	3.1
Methyl 6-O-methyl-β-D-glucopyranoside (**12**)								
Obsd.	1.15	2.5	5.45	2.1	1.0	2.45	6.2	2.0
Calcd	1.8	4.6	5.5	2.4	0.8	5.7	4.1	2.0
Methyl α-D-galactopyranoside (**13**)								
Obsd.	1.1	4.9	6.2	5.7	0.9	3.7	8.3	4.0
Calcd	1.7	2.9	8.3	4.2	2.5	2.8	8.2	4.7
Methyl β-D-galactopyranoside (**14**)								
Obsd.	1.1	4.8	6.6	5.5	1.45	3.95	7.6	4.4
Calcd	2.0	1.6	9.8	4.3	2.5	2.0	9.3	4.7
Methyl 6-O-methyl-α-D-galactopyranoside (**15**)								
Obsd.	1.1	3.4	6.85	5.2	0.9	3.05	7.15	4.75
Calcd	1.7	2.9	8.3	4.2	2.5	2.8	8.2	4.7
Methyl 6-O-methyl-β-D-galactopyranoside (**16**)								
Obsd.	1.45	2.95	8.25	4.35	1.5	3.2	6.9	4.8
Calcd	2.0	1.6	9.8	4.3	2.5	2.0	9.3	4.7

[a] Proton–proton and carbon–proton couplings of **9**–**16** rotamers were calculated from the B3LYP/6-31G** optimized geometries using modified Karplus equations[31] and Eq. (1)[32], respectively.

phase, the *gg* rotamer is the dominant species and that the stability the hydroxymethyl rotamers is in the order of $gg \gg tg > gt$. As expected from the free energy values in Table 6, the rotamer equilibrium in solution is significantly different. It can be seen that the population of the *gt* rotamer increases with the solvent polarity. An increase in the population of the *gt* rotamer is mainly at the expense of the *gg* rotamer with a slight decrease in the *tg* rotamer population, and in water the populations of the *gg* and *gt* rotamers are very similar. The effect of replacement of HO-6 by a methoxy group is a change of conformational behavior around the C-5–C-6 linkage in **11** and **12** compared to **9** and **10**. The main difference is a large stabilization of the *tg* relative to the *gg* rotamer. For **11** and **12**, the C-6 methoxy group cannot act as a hydrogen bond donor which destablizes the counterclockwise hydrogen bonding network, presumably causing the increase in the relative energy of the *gg* rotamer. For 6-*O*-methyl glucopyranosides **11** and **12**, data in Table 9 reveal the major differences in the rotamer populations when going from the gas phase to solution. In vacuum, the *gt* rotamer is the dominant rotamer. The solvent effects noticeably increases the population of the *gg* rotamer at the expense of *gt* and *tg* rotamers. As a result, in aqueous solution the *gg* rotamer is preferred for **11** and **12**. For example, in **11** the calculated population of the *gg* rotamer increases from 23% in the gas phase, through 37% in methanol to 68% in water.

Conformational preferences around the C-5–C-6 bond in the galactopyranose derivatives **13**–**16** display different behavior compared to glucopyranose derivatives **9**–**12**. For **13** and **14**, there is no a dominant rotamer in the gas phase and the population distribution of *gg*, *gt*, and *tg* rotamers was calculated to be 44:12:44 and 30:30:40, respectively. However, solvent

effects considerably change the rotamer equilibrium. In solution, the population of the *gt* rotamer appreciably increases and in aqueous solution the *gt* rotamer is preferred (~ 70%). The effect of methylation of O-6, going from **13** (**14**) to **15** (**16**), results in a larger population of the *gt* rotamer in the gas phase and this conformer is the preferred rotamer, especially in **16**. It appears that solvent effect on a distribution of rotamers of **15** and **16** is smaller compared to the effect on **13** and **14**. The main effect is a slight increase of the *tg* rotamer. Similarly as in the case of **1**–**8**, the results for **9**–**16** suggest that from four major effects assumed to influence the conformational preferences around the C-5–C-6 bond, the gauche effect, hydrogen bonding, steric interactions and solvent effects; the gauche preference of the hydroxymethyl group being mainly due to solvent effects and to the presence of hydrogen bonding and not due to the intrinsic stereoelectronic gauche effect.

Table 7
Relative energies (ΔE, kcal/mol), free energies in vacuum (ΔG_{gas}), methanol (ΔG_M) and aqueous solution (ΔG_W) and observed hydrogen bonds calculated for **9**–**16** using the B3LYP/6-311++G**//6-31G** method

Rotamer	ΔE	ΔG_{gas}	ΔG_M	ΔG_W	ΔE	ΔG_{gas}	ΔG_M	ΔG_W
	Methyl α-D-glucopyranoside (**9**)				Methyl β-D-glucopyranoside (**10**)			
gg_CC	0.26	0.00	0.00	0.00	0.00	0.00	0.00	0.00
gg_C	3.21	2.55	1.23	0.84	2.58	2.47	0.22	0.17
gt_CC	2.36	1.31	0.43	0.14	2.11	1.24	0.29	0.02
gt_C	4.47	3.71	1.41	0.75	3.84	3.40	0.97	0.62
tg_CC	0.00 [a]	1.03	1.63	1.82	0.00 [b]	1.34	1.95	2.02
tg_C	3.20	2.89	1.68	1.92	3.34	3.69	1.78	1.88
	Methyl 6-*O*-methyl-α-D-glucopyranoside (**11**)				Methyl 6-*O*-methyl-β-D-glucopyranoside (**12**)			
gg_CC	0.66	0.51	0.08	0.00	0.74	0.82	0.00	0.00
gg_C	3.04	2.82	1.65	2.39	3.41	3.93	3.18	3.21
gt_CC	0.34	0.00	0.00	0.66	0.00 [d]	0.00	0.00	0.39
gt_C	4.85	3.95	1.12	1.50	5.53	5.02	1.66	5.93
tg_CC	2.07	1.23	0.80	1.99	3.72	3.53	2.92	4.35
tg_C	0.00 [c]	0.61	0.98	1.90	0.62	1.35	1.46	2.26
	Methyl α-D-galactopyranoside (**13**)				Methyl β-D-galactopyranoside (**14**)			
gg_CC	0.45	0.56	0.38	0.98	0.67	1.01	0.90	0.36
gg_C	1.34	1.61	2.21	2.57	1.10	1.79	1.96	1.35
gt_CC	0.00 [e]	0.00	0.00	0.00	0.00 [f]	0.00	0.00	0.00
gt_C	4.71	4.01	1.21	1.43	4.53	4.02	0.44	0.03
tg_CC	0.27	0.36	1.31	1.82	0.20	0.70	1.72	1.59
tg_C	4.09	3.72	2.17	2.20	4.24	4.23	1.86	1.07
	Methyl 6-*O*-methyl-α-D-galactopyranoside (**15**)				Methyl 6-*O*-methyl-β-D-galactopyranoside (**16**)			
gg_CC	5.10	3.17	1.06	0.94	4.77	4.42	1.26	0.99
gg_C	2.26	0.35	1.13	1.11	0.59	1.37	1.68	1.27
gt_CC	0.00 [g]	0.00	0.00	0.00	0.00 [h]	0.00	0.00	0.00
gt_C	6.03	5.46	2.98	2.83	4.53	3.64	0.06	0.26
tg_CC	1.56	0.87	1.93	0.63	0.13	1.29	2.21	0.74
tg_C	2.44	1.21	1.08	1.29	1.10	2.37	0.80	0.97

[a] $E = -726.714464$.
[b] $E = -726.712665$.
[c] $E = -766.022564$.
[d] $E = -766.021115$.
[e] $E = -726.713182$.
[f] $E = -726.711359$.
[g] $E = -766.019888$.
[h] $E = -766.017618$.

Table 8
Torsional angles calculated at the B3LYP/6-31G** level and the corresponding $^3J_{C\text{-}4\text{–}H\text{-}6}$ and $^3J_{H\text{-}5\text{–}H\text{-}6}$ coupling constants determined using Karplus-like equations[31,32] for the rotamers of **9–16**

Conformers	$\chi_{C\text{-}4\text{–}H\text{-}6R}$	$^3J_{C\text{-}4\text{–}H\text{-}6R}$	$\chi_{C\text{-}4\text{–}H\text{-}6S}$	$^3J_{C\text{-}4\text{–}H\text{-}6S}$	$\chi_{H\text{-}5\text{–}H\text{-}6R}$	$^3J_{H\text{-}5\text{–}H\text{-}6R}$	$\chi_{H\text{-}5\text{–}H\text{-}6S}$	$^3J_{H\text{-}5\text{–}H\text{-}6S}$
Methyl α-D-glucopyranoside ***(9)***								
gg_CC	−59.0	1.00	−179.1	7.93	68.0	0.52	−49.9	4.04
gg_C	−60.8	0.90	−178.4	7.93	67.5	0.53	−50.4	4.04
gt_CC	54.3	1.81	−63.7	0.75	−172.7	9.97	70.4	2.06
gt_C	53.6	1.86	−64.7	0.70	175.7	10.96	57.3	3.36
tg_CC	169.7	7.61	53.4	1.88	−64.3	4.26	178.1	10.66
tg_C	−179.8	7.92	62.3	1.24	−55.1	5.77	−173.1	10.58
Methyl β-D-glucopyranoside ***(10)***								
gg_CC	−54.8	1.28	−173.0	7.89	66.9	0.55	−51.6	3.78
gg_C	−61.2	0.88	−178.9	7.93	66.7	0.55	−51.6	3.78
gt_CC	55.8	1.70	−61.9	0.84	−170.7	9.73	72.0	1.94
gt_C	54.4	1.80	−63.7	0.75	173.5	11.07	55.3	3.67
tg_CC	169.1	7.58	52.4	1.96	−64.6	4.26	178.2	10.66
tg_C	−179.2	7.93	63.1	1.19	−55.3	5.77	−173.3	10.58
Methyl 6-O-methyl-α-D-glucopyranoside ***(11)***								
gg_CC	−65.2	0.67	177.4	7.88	54.3	1.58	−63.0	2.58
gg_C	−79.1	0.34	163.6	7.24	41.0	3.24	−76.3	1.57
gt_CC	70.5	0.79	−47.6	1.81	−168.7	9.59	73.2	1.86
gt_C	66.5	0.99	−51.0	1.55	173.2	11.18	69.2	2.16
tg_CC	149.7	5.97	32.2	3.56	−88.2	1.51	154.3	9.02
tg_C	−179.2	7.93	62.7	1.22	−58.3	5.17	176.4	10.74
Methyl 6-O-methyl-β-D-glucopyranoside ***(12)***								
gg_CC	−64.3	0.72	177.7	7.89	54.3	1.58	−63.3	2.55
gg_C	−79.8	0.34	163.0	7.19	40.2	3.36	−77.3	1.53
gt_CC	70.0	0.81	−47.7	1.81	−169.9	9.75	72.4	1.91
gt_C	72.0	0.72	−45.6	1.97	−168.0	9.50	74.4	1.78
tg_CC	122.6	2.79	4.6	4.73	−116.2	1.71	125.8	4.74
tg_C	−178.7	7.93	63.4	1.17	−57.8	5.24	−175.8	10.75
Methyl α-D-galactopyranoside ***(13)***								
gg_CC	−60.4	0.92	−177.3	7.93	57.4	1.10	−59.1	2.95
gg_C	−52.5	1.44	−172.0	7.87	67.6	0.52	−51.9	3.80
gt_CC	55.6	1.71	−63.1	0.78	176.4	10.90	57.5	3.30
gt_C	55.0	1.76	−63.6	0.75	175.9	10.96	57.3	3.42
tg_CC	−153.3	6.81	89.4	0.49	−33.4	8.47	−150.7	8.71
tg_C	−165.4	7.64	77.1	0.55	−44.9	7.07	−162.4	10.00
Methyl β-D-galactopyranoside ***(14)***								
gg_CC	−60.8	0.90	−177.4	7.93	56.8	1.13	-59.9	2.84
gg_C	−52.3	1.46	−172.2	7.88	67.7	0.52	-52.2	3.78
gt_CC	54.2	1.82	−64.6	0.70	174.5	11.07	55.7	3.54
gt_C	52.9	1.92	−66.1	0.63	173.2	11.16	54.8	3.67
tg_CC	−157.6	7.16	85.3	0.45	−38.1	8.06	−155.2	9.20
tg_C	−167.1	7.72	75.5	0.60	−46.5	6.94	−163.9	10.08
Methyl 6-O-methyl-α-D-galactopyranoside ***(15)***								
gg_CC	−54.6	1.29	169.9	7.62	62.1	1.00	−53.2	2.84
gg_C	−65.3	0.67	176.8	7.87	52.5	0.52	−65.4	3.80
gt_CC	70.1	0.81	−48.2	1.77	−171.1	10.90	70.7	3.30
gt_C	65.6	1.04	−51.8	1.49	−175.6	10.96	66.9	3.42
tg_CC	176.5	7.86	59.1	1.46	−62.8	8.47	179.8	8.71
tg_C	161.9	7.11	80.2	0.49	−41.2	7.07	−159.1	10.00

Table 8 (*Continued*)

Conformers	$\chi_{C\text{-}4\text{–}H\text{-}6R}$	$^3J_{C\text{-}4\text{–}H\text{-}6R}$	$\chi_{C\text{-}4\text{–}H\text{-}6S}$	$^3J_{C\text{-}4\text{–}H\text{-}6S}$	$\chi_{H\text{-}5\text{–}H\text{-}6R}$	$^3J_{H\text{-}5\text{–}H\text{-}6R}$	$\chi_{H\text{-}5\text{–}H\text{-}6S}$	$^3J_{H\text{-}5\text{–}H\text{-}6S}$
Methyl 6-O-methyl-β-D-galactopyranoside (**16**)								
gg_CC	−53.6	1.36	−169.9	7.82	63.2	1.13	−53.1	2.84
gg_C	−67.2	0.59	174.7	7.81	50.7	0.52	−67.5	3.78
gt_CC	64.8	1.09	−52.8	1.42	−176.8	11.07	65.5	3.54
gt_C	56.6	1.64	−60.9	0.89	175.3	11.16	57.8	3.67
tg_CC	174.7	7.81	57.7	1.56	−64.9	8.06	178.1	9.20
tg_C	164.1	7.27	77.9	0.53	−43.6	6.94	−161.5	10.08

In general, an agreement between the *gg*, *gt*, and *tg* rotamer populations calculated and estimated from NMR data is very good. The calculations describe well the shift in the rotamer populations going from the gas phase to methanol and to aqueous solution. We would like to emphasize that we have not attempted to scan the entire conformational surface of **9**–**16**. The conformations of **9**–**16** used for calculations correspond to only on a very small fraction of such a conformational energy surface. In fact, selected conformers represent gas phase structures whose preference is largely due to maximization of intramolecular hydrogen bonds and these hydrogen patterns may change in solution where intermolecular hydrogen bonds must also be accommodated. Therefore, the agreement of the predicted values for populations of the hydroxymethyl and methoxymethyl rotamers of **9**–**16** in two solvents with those determined from the analysis of vicinal proton–proton couplings is slightly surprising and might be fortuitous. On the other hand, these results indicate that the method used for calculations of solvent effects provide reasonable estimates. However, it appears that the rotamer populations estimated from the carbon–proton coupling (the $^3J_{CH}$ rows in Table 7) exhibit a larger discrepancy with the calculated and other experimental values. For **9**–**12**, they usually display higher populations of the *gt* rotamer. This trend is more pronounced in methyl glucopyranosides **9**–**12**, while in methyl galactopyranosides **13**–**16** the prediction is reasonable.

The accuracy of the analysis of the rotamer populations depends on several factors that have been recently thoroughly discussed.[2,3] The negative *tg* rotamer populations in Table 9 are results of mathematical analysis of data and reflect either incorrect values of the limiting vicinal coupling constants ($^3J_{HH}$ or $^3J_{CH}$) in *gg*, *gt*, and *tg* rotamers or inaccuracy in the experimental measurements.[2,3] Here the limiting values used for calculations of the rotamer populations were based on the optimized values of torsional angles (Table 8). These values were also used to calculate the average values of $^3J_{H\text{-}5\text{–}H\text{-}6R}$, $^3J_{H\text{-}5\text{–}H\text{-}6S}$, $^3J_{C\text{-}4\text{–}H\text{-}6R}$, and $^3J_{C\text{-}4\text{–}H\text{-}6S}$ coupling constants that are listed in Table 6. Again, the larger differences between the experimental and calculated values are observed for $^3J_{CH}$ constants, especially $^3J_{C\text{-}4\text{–}H\text{-}6S}$. The intrinsic nature of the conformational dependence of vicinal couplings might explain these differences. The values of vicinal coupling constant are very sensitive to a change of values of torsional angles, especially in a region of gauche conformations. For example, an inspection of the values in Table 8 revealed that the $\chi_{C\text{-}4\text{–}H\text{-}6R}$ torsional angle adopts for the *gg* rotamers values in the range from −52 to −80°. The corresponding values of $^3J_{CH}$ are 1.43 and 0.34 Hz, respectively. This example illustrates how a small inaccuracy in torsional angles used for the estimation of $^3J_{CH}$ or $^3J_{HH}$ values might influence the rotamer populations. Since the external hydrogen bonds were not taken into account during the optimization of geometry, the calculated torsional angles of the **9**–**16** rotamers in solution may have slightly different values than those listed in Table 8. This assumption is supported by a comparison of the calculated ω angle (O-5–C-5–C-6–O-6) and from solid state. Average angles from 101 structures with gluco configuration were −66.5° for the *gg* rotamer and +65.0° for the *tg* rotamer.[4] The ω torsional angles calculated here were from −55 to −70° for the *gg* rotamer, from 65 to 75° for the *gt* rotamer, and from −172 to 178° for the *tg* rotamer, respectively. This clearly illustrates that the torsional angles are far from those in ideal staggered orientations and proper calculations would require incorporating changes of torsional angles due to direct interactions between solvent and hexopyranose. Performing solvated molecular dynamics with a properly parameterized force field can do this.[9,10,26]

In conclusion, the results of conformational analysis of **1**–**16** obviously showed that the populations of the *gg*, *gt*, and *tg* rotamers in the gas phase and solution differ considerably. Moreover, a correct prediction of the rotamer populations in solution has been obtained only when solvent contributions were included into calculations. Finally, the results clearly demonstrate that the gauche preference of the O-5–C-5–C-6–O-6 structural moiety is due to the intramolecular hydrogen bonding and solvent effects and not due to an intrinsic stereoelectronic effect known as the gauche effect.[51]

Table 9
Rotamer populations of compounds **9**–**16** in the gas phase, in methanol and aqueous solution estimated from the free energies ΔG_{gas}, ΔG_M, and ΔG_W calculated using the B3LYP/6-311++G** method

	Reference	*GG*	*GT*	*TG*	*GG*	*GT*	*TG*
		Methyl α-D-glucopyranoside (**9**)			Methyl β-D-glucopyranoside (**10**)		
Gas phase	Calcd	77.5	8.5	14.0	81.4	10.1	8.5
Methanol	2	56	51	−7			
	$^3J_{CH}$	27	80	−7	24	81	−5
	$^3J_{HH}$	62	53	−15	59	56	−15
	Calcd	61.7	31.6	6.7	65.4	31.2	3.4
Water	39	57	38	5			
	5	58	38	4	50	47	3
	5	59	49	−8	51	58	−9
	5	59	41	0	51	49	0
	2	57	50	−7	50	56	−6
	3	48	48	4			
	$^3J_{CH}$	31	76	−7	23	85	−8
	$^3J_{HH}$	65	53	−18	50	62	−13
	Calcd	51.8	44.7	3.5	55.7	41.9	2.4
		Methyl 6-*O*-methyl-α-D-glucopyranoside (**11**)			Methyl 6-*O*-methyl-β-D-glucopyranoside (**12**)		
Gas phase	Calcd	22.5	52.3	25.2	18.6	73.7	7.7
Methanol	$^3J_{CH}$	5	93	2	11	83	6
	$^3J_{HH}$	67	47	−14	48	48	3
	Calcd	36.9	45.4	17.7	46.6	49.1	4.3
Water	5	70	29	1	56	41	3
	$^3J_{CH}$	19	76	5	10	87	3
	$^3J_{HH}$	65	42	−7	40	58	2
	Calcd	67.8	27.2	5.0	65.0	33.5	1.5
		Methyl α-D-galactopyranoside (**13**)			Methyl β-D-galactopyranoside (**14**)		
Gas phase	Calcd	43.7	12.0	44.3	29.8	30.4	39.8
Methanol	$^3J_{CH}$	57	46	−3	57	47	−4
	$^3J_{HH}$	36	19	45	33	28	38
	Calcd	23.2	50.8	26.1	17.8	55.3	26.9
Water	39	14	47	39			
.	5	21	61	18	22	55	23
	5	13	70	17	17	65	18
	5	15	69	16	15	64	21
	$^3J_{CH}$	40	69	-9	45	54	1
	$^3J_{HH}$	23	63	14	29	53	18
	Calcd	14.5	71.6	13.9	11.8	75.9	12.3
		Methyl 6-*O*-methyl-α-D-galactopyranoside (**15**)			Methyl 6-*O*-methyl-β-D-galactopyranoside (**16**)		
Gas phase	Calcd	29.1	52.1	18.8	8.1	81.3	10.7
Methanol	$^3J_{CH}$	28	69	3	31	72	−3
	$^3J_{HH}$	31	35	33	16	69	15
	Calcd	20.7	66.2	13.1	7.5	80.5	12.0
Water	5	16	53	31	12	64	24
	$^3J_{CH}$	22	77	1	34	67	−1
	$^3J_{HH}$	30	44	26	26	54	20
	Calcd	19.6	55.3	25.1	12.6	67.6	19.8

Thermodynamics and solvent effect contributions were calculated at the B3LYP/6-31G** level.

References

1. Dennis, J. W.; Laferte, S.; Waghorne, C.; Breitman, M. L.; Kerbel, R. S. *Science* **1987**, *236*, 582–585.
2. Bock, K.; Duus, J. O. *J. Carbohydr. Chem.* **1994**, *13*, 513–543.
3. Rockwell, G. D.; Grindley, T. B. *J. Am. Chem. Soc.* **1998**, *120*, 10953–10963.
4. Marchessault, R. H.; Perez, S. *Biopolymers* **1979**, *18*, 2369–2374.
5. Nishida, Y.; Hori, H.; Ohrui, H.; Meguro, H. *J. Carbohydr. Chem.* **1988**, *7*, 239–250.
6. Tvaroška, I.; Kozár, T. *Theor. Chem. Acta* **1986**, *70*, 99–114.
7. De Vries, N. K.; Buck, H. M. *Carbohydr. Res.* **1987**, *165*, 1–16.
8. Darsey, J. A.; Voll, R. J.; Younathan, E. S.; Koerner, T. A. W., Jr. *Carbohydr. Res.* **1988**, *173*, 197–204.
9. Kroon-Batenburg, L. M. J.; Kroon, J. *Biopolymers* **1990**, *29*, 1243–1248.
10. Ha, S.; Gao, J.; Tidor, B.; Brady, J. W.; Karplus, M. *J. Am. Chem. Soc.* **1991**, *113*, 1553–1557.
11. Zheng, Y.-J.; Le Grand, S. M.; Merz, K. M., Jr. *J. Comput. Chem.* **1992**, *13*, 772–791.
12. Polavaru, P. L.; Ewing, C. S. *J. Comput. Chem.* **1992**, *13*, 1255–1261.
13. Cramer, C. J.; Truhlar, D. G. *J. Am. Chem. Soc.* **1993**, *115*, 5745–5753.
14. Salzner, U.; Schleyer, P.v. R. *J. Org. Chem.* **1994**, *59*, 2138–2155.
15. Woods, R. J.; Dwek, R. A.; Edge, C. J.; Fraser-Reid, B. *J. Phys. Chem.* **1995**, *99*, 3832–3846.
16. Barrows, S. E.; Dulles, F. J.; Cramer, C. J.; French, A. D.; Truhlar, D. G. *Carbohydr. Res.* **1995**, *276*, 219–251.
17. Brown, J. W.; Wladkowski, B. D. *J. Am. Chem. Soc.* **1996**, *118*, 1190–1193.
18. Tvaroška, I.; Carver, J. P. *J. Phys. Chem. B* **1997**, *101*, 2992–2999.
19. Csonka, G. I.; Elias, K.; Csizmadia, I. G. *Chem. Phys. Lett.* **1996**, *257*, 49–60.
20. Damm, W.; Frontera, A.; Tirado-Rives, J.; Jorgensen, W. L. *J. Comput. Chem.* **1997**, *18*, 1955–1970.
21. Molteni, C.; Perrinello, M. *J. Am. Chem. Soc.* **1998**, *120*, 2168–2171.
22. Ma, B.; Schaefer, H. F., III; Allinger, N. L. *J. Am. Chem. Soc.* **1998**, *120*, 3411–3422.
23. Simmerling, C.; Fox, T.; Kollman, P. *J. Am. Chem. Soc.* **1998**, *120*, 5771–5782.
24. Li, J.-H.; Ma, B.; Allinger, N. L. *J. Comput. Chem.* **1999**, *20*, 1593–1603.
25. Stenger, J.; Cowman, M.; Eggers, F.; Eyring, E. M.; Katze, U.; Petrucci, S. *J. Phys. Chem. B* **2000**, *104*, 4782–4790.
26. Kirschner, K. N.; Woods, R. J. *Proc. Nat. Acad. Sci. USA* **2001**, *98*, 10541–10545.
27. JAGUAR 3.5, S., Schrodinger, Inc., Portland, 1998.
28. Becke, A. D. *J. Chem. Phys.* **1993**, *98*, 5648–5652.
29. Parr, R. G.; Yang, W. *Density-Functional Theory of Atoms and Molecules*; Oxford University: New York, 1989.
30. Tannor, D. J.; Marten, B.; Murphy, R.; Friesner, R. A.; Sitkoff, D.; Nicholls, A.; Ringnalda, M.; Goddard, W. A., III; Honig, B. *J. Am. Chem. Soc.* **1994**, *116*, 11875–11882.
31. Haasnoot, C. A. G.; DeLeeuw, F. A. A. M.; Altona, C. *Tetrahedron* **1980**, *36*, 2783–2792.
32. Tvaroška, I.; Gajdoš, J. *Carbohydr. Res.* **1995**, *271*, 151–162.
33. Timell, T. E.; Enterman, W.; Spencer, F.; Soltes, E. J. *Can. J. Chem.* **1965**, *43*, 2296–2305.
34. Cadotte, J. E.; Dutton, G. G. S.; Goldstein, I. J.; Lewis, B. A.; Smith, F.; Van Cleve, J. W. *J. Am. Chem. Soc.* **1957**, *79*, 691–695.
35. Kent, P. W.; Morris, A.; Taylor, N. F. *J. Chem. Soc.* **1960**, 298–303.
36. Usov, A. I.; Kozlova, E. G. *Bioorg. Khim.* **1975**, *1*, 912–918.
37. De Bruyn, A.; Anteunis, M. *Carbohydr. Res.* **1976**, *47*, 311–314.
38. Nardin, R.; Saint-Germain, J.; Vincendon, M.; Taravel, F. R.; Vignon, M. R. *Nouv. J. Chim.* **1984**, *8*, 305–309.
39. Nishida, Y.; Ohrui, H.; Meguro, H. *Tetrahedron Lett.* **1984**, *25*, 1575–1578.
40. Ohrui, H.; Nishida, Y.; Higuchi, H.; Hori, H.; Meguro, H. *Can. J. Chem.* **1987**, *65*, 1145–1153.
41. Gagnaire, D.; Horton, D.; Taravel, F. R. *Carbohydr. Res.* **1973**, *27*, 363–372.
42. Gagnaire, D.; Taravel, F. R. *FEBS Lett.* **1975**, *60*, 317–321.
43. Ohrui, H.; Nishida, Y.; Watanabe, M.; Hori, H.; Meguro, H. *Tetrahedron Lett.* **1985**, *27*, 3251–3254.
44. Aue, W. P.; Bartholdi, E.; Ernst, R. R. *J. Chem. Phys.* **1976**, *64*, 2229–2246.
45. Harris, R. K. In *Nuclear Magnetic Resonance Spectroscopy*; Harris, R. K., Ed.; Longman Group: Harlow, 1986; pp. 165–187.
46. Bohenhausen, G.; Freeman, R.; Morris, G. A. *J. Magn. Reson.* **1976**, *23*, 171–175.
47. Morat, C.; Taravel, F. R.; Vignon, M. R. *Carbohydr. Res.* **1987**, *163*, 265–268.
48. Bax, A.; Freeman, R. *J. Am. Chem. Soc.* **1982**, *104*, 1099–1100.
49. Behrends, R.; Cowman, M. K.; Eggers, F.; Eyring, E. M.; Kaatze, U.; Majewski, J.; Petrucci, S.; Richmann, K.-H.; Riech, M. *J. Am. Chem. Soc.* **1997**, *119*, 2182–2186.
50. Tvaroška, I.; Bleha, T. *Adv. Carbohydr. Chem. Biochem.* **1989**, *47*, 45–123.
51. Wolfe, S. *Acc. Chem. Res.* **1972**, *5*, 102–111.
52. Tvaroška, I.; Taravel, F. R. *Adv. Carbohydr. Chem. Biochem.* **1995**, *51*, 15–61.